

1 Breakthrough technologies

2

3 Short title: High efficiency *Cuscuta* transformation

4

5 **A highly efficient protocol for transforming *Cuscuta reflexa* based on**
6 **artificially induced infection sites**

7

8 **Authors:** Lena Anna-Maria Lachner, Levon Galstyan[†] and Kirsten Krause¹

9

10 **Affiliations:**

11 Department of Arctic and Marine Biology, UiT The Arctic University of Norway, 9037

12 Tromsø, Norway

13 [†]Current address: Faculty of Food Technologies, Teryan 74, Armenian National Agrarian

14 University, 0009 Yerevan, Armenia

15

16 ¹Author for contact: kirsten.krause@uit.no

17

18 **Author contributions:** L.G. and K.K. designed the transformation setup; L.L. and L.G.
19 performed the transformation experiments; L.L. performed the life cell staining experiments,
20 evaluated all data and performed image analyses; K.K. conceived the project and wrote the article
21 with contributions of all the authors.

22 **Funding information:** The work was funded by the Tromsø Research Foundation (grant 16-TF-
23 KK to K. K.), UiT The Arctic University of Norway (PhD stipend to L. L.) and the Norwegian
24 Agency for International Cooperation and Quality Enhancement in Higher Education (DIKU)
25 (Eurasia program grant CPEA-LT-2016/10092, supporting a research visit by L. G. to Tromsø).

26 **ONE SENTENCE SUMMARY**

27 A protocol that yields high numbers of transformed cells in the adhesive disks of *Cuscuta reflexa*
28 upon exposure to agrobacteria brings closer the vision of generating genetically modified
29 *Cuscuta*.

30

31 **ABSTRACT**

32 A current bottleneck in the functional analysis of the emerging parasitic model plant *Cuscuta* and
33 the exploitation of its recently sequenced genomes is the lack of efficient transformation tools.
34 Here, we describe the development of a novel highly efficient *Agrobacterium*-mediated
35 transformation protocol for *Cuscuta reflexa* based on the parasitic structure referred to as
36 adhesive disk. Both, *Agrobacterium rhizogenes* and *Agrobacterium tumefaciens* carrying binary
37 transformation vectors with reporter fluorochromes yielded high numbers of transformation
38 events. An overwhelming majority of transformed cells were observed in the cell layer below the
39 adhesive disk's epidermis, suggesting that these cells are particularly susceptible to infection. Co-
40 transformation of these cells happens frequently when *Agrobacterium* strains carrying different
41 constructs are applied together. Explants containing transformed tissue expressed the fluorescent
42 markers in *in vitro* culture for several weeks, offering a possibility for development of
43 transformed cells into callus.

44

45

46

47 **INTRODUCTION**

48 The obligate parasitic plant genus *Cuscuta*, commonly known as “dodder”, is found almost
49 worldwide and infects a broad range of host plants. The parasite starts an attack by winding
50 around the host stem. A multicellular feeding structure termed the haustorium, which can reach
51 2-3 mm in size in some species and originates from a secondary meristem in the cortex close to
52 the vascular bundles, develops within a few days and breaches the host tissue integrity using
53 mechanical pressure and enzymatic digestion of cell walls (Nagar et al., 1984; Johnsen et al.,
54 2015; Kaiser et al., 2015). To make the penetration possible, a sucker-shaped attachment organ
55 provides the necessary counterforce. The development of this organ, termed “adhesive disk” or
56 “upper haustorium” (Vaughn, 2002; Lee, 2007; Kaiser et al., 2015), is easily visible as a swelling
57 of the host-facing side of the parasite’s stem. A bio-adhesive, secreted by the epidermal cells of
58 the adhesive disk, anchors the parasite to the host (Vaughn, 2002; Galloway et al., 2020).
59 Morphologically, the development of the adhesive disk is marked by major local growth
60 processes and shape changes of the involved cells: on one hand elongation of cells in the
61 parasite’s cortex around the developing haustorium takes place; on the other hand, an even more
62 drastic reconfiguration of the epidermis into digitate or club-shaped cells can be noted (Shimizu
63 and Aoki, 2019).

64 In light of the detrimental effect to important crops exerted by *Cuscuta* worldwide, it is
65 imperative, that mechanisms guiding the parasitic attack are better understood. One prerequisite
66 for achieving a better understanding of the molecular processes and mechanisms of a *Cuscuta*
67 attack is a reference genome. Recently, complete genome sequences have been published for two
68 *Cuscuta* species, *C. campestris* and *C. australis* (Sun et al., 2018; Vogel et al., 2018). However,
69 two significant bottlenecks to perform targeted genome manipulations remain in the form of low
70 transformation efficiency and poor regeneration rates of *Cuscuta* tissues *in vitro*. Some few
71 approaches to transform *C. trifolii* (Borsics et al., 2002) and *C. europaea* (Svubova and Blehova,

72 2013) have been reported. Explants from seedlings were transformed using *Agrobacterium*
73 *tumefaciens*, and expression of the transgenes was demonstrated in the calli. However, the
74 generation of a whole transgenic *Cuscuta* plant has to date not been reported, indicating that the
75 current techniques lack efficiency.

76 Besides *A. tumefaciens*, *Agrobacterium rhizogenes* has become a popular agent for transforming
77 plant genomes (Ozyigit et al., 2013). *A. rhizogenes* is a soil-borne bacterium infecting many
78 angiosperms and causing them to produce a copious number of roots which became known as the
79 “hairy root syndrome” (Bahramnejad et al., 2019). Like *A. tumefaciens*, *A. rhizogenes* transfers a
80 segment of DNA known as T-DNA into its hosts. The transfer process is controlled by virulence
81 (*vir*) genes that are induced by phenolic signal molecules (Gelvin, 2003). The *A. rhizogenes* T-
82 DNA is stably integrated into the plant nuclear genome where it expresses the *rol* (*rooting locus*)
83 genes required for excessive adventitious root growth (Ozyigit et al., 2013). What has made these
84 hairy roots popular for plant biotechnology is that they can be propagated in the absence of
85 exogenous plant hormones. Very recently, it was shown that an *A. rhizogenes* gene coding for the
86 mikimopine synthase was horizontally transferred into several *Cuscuta* species (Zhang et al.,
87 2020), including *Cuscuta campestris* (Vogel et al., 2018) and *Cuscuta australis* (Sun et al.,
88 2018), suggesting that *Cuscuta* species may be susceptible to infection by this *Agrobacterium*
89 species despite their lack of roots.

90 With this study, we set out to test the applicability of the hairy root transformation protocol in
91 *Cuscuta*. Although hairy roots as such were not obtained, we were able to obtain high numbers of
92 transformed cells in the species *Cuscuta reflexa*, particularly in its adhesive disks. We describe
93 here the simple and highly efficient protocol that can yield hundreds of transformed cells within a
94 week based on the use of *A. rhizogenes*. We further show that the protocol is applicable to use
95 with *A. tumefaciens* with equally high success, which widens possibilities for single or co-
96 transformation of different constructs. Our trials with other *Cuscuta* species showed some
97 transformation success but were not as reliable as experiments with *C. reflexa*. Although some

98 species-specific adaptations may be required, our protocol is overall fast, flexible, easily scalable
99 and suitable for transformations of genes at high throughput, and a first step towards making
100 *Cuscuta* amenable to genome modifications.

101

102 RESULTS

103 *Agrobacterium rhizogenes* does not induce hairy roots in *Cuscuta* species

104 *A. rhizogenes* is typically applied to the roots (Ho-Plagaro et al., 2018), hypocotyl (Alagarsamy et
105 al., 2018) or cotyledons (Ron et al., 2014) of dicotyledonous angiosperms by cutting, puncturing
106 or otherwise wounding these tissues. In the absence of proper roots, cotyledons or other leaves,
107 we first tested hairy root induction on young germinating seedlings of *C. campestris* and on
108 different parts of the shoots from different *Cuscuta* species using *A. rhizogenes* with and without
109 the pRedRoot T-DNA. Occasionally, transformed cells exhibiting an intense orange fluorescence
110 from expression of the reporter protein dsRed have indeed been observed, particularly in shoot
111 tips (Supplemental Fig. S1). However, no root development could be observed in any of our trials
112 with the strain MSU440, independent of whether it carried the pRedRoot T-DNA or not and
113 transformation success reliability was poor.

114

115 *A. rhizogenes* transforms adhesive disk cells of *C. reflexa* with high efficiency

116 We next decided to expose developing infection structures to a pRedRoot-containing *A.*
117 *rhizogenes* culture. For this we used the method for induction of haustoriogenesis in *C. reflexa*
118 described by Olsen et al. (2016) that uses a combination of far-red light illumination and tactile
119 stimuli to synchronize haustorial development (Tada et al., 1996). The stems on which the
120 infection sites developed were exposed to *A. rhizogenes* for as long as it took for haustoria to
121 emerge (7-8 days) (Fig. 1). Upon microscopical analysis, a large number of intensely orange-
122 fluorescing cells expressing dsRed were revealed that were almost exclusively located in the

123 adhesive disks around the protruding haustorium (Fig. 2A-F). The dsRed fluorescence was
124 visible in distinct spots often consisting of 5-15 clustered cells, but single transformed cells and
125 bigger clusters were also observed (Fig. 2). Cross sections through sites where transformation had
126 occurred revealed that the cells expressing the dsRed were mostly not located at the very surface
127 but rather in a cell layer directly below the elongated epidermal cells (Fig. 2G-L). 52 % of the
128 adhesive disks exhibited one or more spots with dsRed fluorescence (based on 52 infected shoots
129 with 426 infection structures) (Table 1), but there was considerable variation between individual
130 shoots. While some green and blue autofluorescence was observed in the central haustorial tissue
131 (Supplemental Fig. S2), the adhesive disk of *C. reflexa* exhibited little to no autofluorescence, as
132 demonstrated by mock transformations with *A. rhizogenes* cells that lack the pRedRoot T-DNA
133 (Fig. 2M, N). Experiments where *A. rhizogenes* was removed or added after 2 days, showed that
134 the uptake of the T-DNA in the first two days is minimal to absent, and seems to happen only
135 once the development of the infection sites has commenced (Supplemental Tab. S1, 2).

136

137 **Adhesive disks readily take up the live cell stain 5-carboxyfluorescein-diacetate (CFDA)**

138 Life cell stains like CFDA are membrane permeable and are hydrolyzed in the cytoplasm to the
139 green fluorescent carboxyfluorescein. Fluorescence inside cells is thus on one hand evidence for
140 their viability and on the other hand reveals which cells lack protection by barriers such as the
141 cuticle that would block uptake of the stain. When shoots that showed dsRed fluorescence in the
142 adhesive disks where exposed to a CFDA solution, the adhesive disks and often (but not always)
143 also the haustoria exhibited green fluorescence (Fig. 3). CFDA fluorescence was also observed
144 regularly in young side-shoot buds but only very rarely in the intact stems (Supplemental Fig.
145 S1). This indicates that the cuticle that protects *Cuscuta* stems and that hinders the uptake of the
146 stain into stems is most likely “leaky” or absent in the adhesive disks and haustoria, thus
147 permitting the stain to enter the respective tissue. This, in turn may explain its susceptibility to
148 agrobacterial infection.

149

150 **Application of the transformation protocol is not limited to *A. rhizogenes***

151 In order to reveal whether the high transformation rates were a result of a specific susceptibility
152 of *C. reflexa* to *A. rhizogenes* we exposed far-red light induced stems to *Agrobacterium*
153 *tumefaciens* carrying a GFP gene in the T-DNA of a binary plasmid (Bobik et al., 2019) using the
154 same setup. Only very weak background fluorescence was seen in this case in the orange channel
155 and in the blue channel, while the high intensity of green fluorescence in a ring corresponding to
156 the adhesive disk indicated that the GFP was expressed in this tissue as a result of the
157 transformation (Fig. 4A-I). As with the dsRed, GFP was expressed in elongated cells beneath the
158 layer of epidermal cells in the adhesive disk (Supplemental Fig. S3). The infection frequency was
159 on average 43% for *A. tumefaciens* (based on 38 infected shoots with 367 infection structures)
160 (Tab. 1).

161

162 **Transformation of other *Cuscuta* species**

163 Within the genus *Cuscuta*, three subgenera are distinguished: subgenus *Monogyna*, which
164 includes *C. reflexa*, subgenus *Grammica* and subgenus *Cuscuta* (Yuncker, 1932). To test whether
165 our protocol is applicable to *C. campestris* whose sequenced genome (Vogel et al., 2018) would
166 make it a very interesting target for genome modifications we repeated the same transformation
167 setup with this species (Fig. 4) and a third *Cuscuta* species, *C. platyloba* (Supplemental Fig. S1),
168 both belonging to the subgenus *Grammica*. With both *Agrobacterium* species, a higher degree of
169 necrotic tissue was observed in these two species as a result of this treatment, which, in turn,
170 created a higher amount of unspecific autofluorescence. While adhesive disk transformation
171 could be observed in *C. campestris* (Fig. 4K-L), it was by far not as frequent as in *C. reflexa* and
172 was often weaker than in stem tissue adjacent to haustoria-forming sites.

173

174 **Simultaneous exposure to both *Agrobacterium* strains yields a high number of co-
175 transformation events**

176 A desired feature of transformation protocols is the possibility to express multiple transgenes in
177 the same cell. This can be achieved by time-consuming sequential transformation or the cloning
178 of suites of genes into the T-DNA of one vector, often yielding large unwieldy constructs.
179 However, the high susceptibility of the same *C. reflexa* tissue to both, *A. rhizogenes* and *A.*
180 *tumefaciens*, opens for the possibility of introducing multiple constructs into the same cell by co-
181 infection. To achieve this, both species of *Agrobacterium* carrying each their respective
182 fluorescent reporter construct (dsRed in *A. rhizogenes* and GFP in *A. tumefaciens*) were mixed in
183 a 1:1 ratio (based on their ODs at 595 nm) prior to exposing the *C. reflexa* stems to them in our
184 transformation setup. Fluorescence microscopy revealed that both, dsRed and GFP were visible
185 with similar yields in the adhesive disks as in single transformation experiments. A considerable
186 amount of overlapping fluorescence indicated that co-transformation did in fact occur at a high
187 rate (Fig. 5A-D). In order to see whether the same cells (and not just cells in the same area)
188 indeed expressed both fluorescent proteins, we prepared semi-thin cross sections through
189 transformed regions and documented the fluorescence location with microphotography (Fig. 5E-
190 H) and by densitometry scanning of fluorescence intensities over an area containing several
191 transformed clusters (Fig. 5I, Supplemental Fig. S4). Both revealed an exact coincidence of the
192 two fluorophores in several cells, suggesting that there are hot spots of susceptible tissue that is
193 frequently co-transformed. At the same time, the occurrence of cells transformed with only one
194 fluorochrome shows that each fluorescence signal is specific.

195

196 **Transgene expression after a transformation event is preserved over several weeks**

197 The frequent occurrence of transformed cell clusters raised the question whether these arose
198 through cell division and propagation of single transformed cells, indicating not only a stable

199 insertion of the transgenes but, moreover, the possibility to regenerate vegetative or reproductive
200 tissue by *in vitro* propagation from the transformation events. To test this, we sterilized explants
201 containing transformed tissue and maintained them in *in vitro* cultures. The explants showed
202 slight growth of cells at the edges of the adhesive disks, including the transformed regions, but
203 significant propagation was not observed over a period of up to 8 weeks. The fluorescence was
204 consistently high for at least 4 weeks (Fig. 6) but started to decreased during longer cultivation
205 times.

206

207 DISCUSSION

208 In the last few years, research on *Cuscuta* has seen a rapid increase and with the publication of
209 the first two genome sequences of *C. campestris* (Vogel et al., 2018) and *C. australis* (Sun et al.,
210 2018), our knowledge on these parasites has experienced a significant leap forward. Nevertheless,
211 there are still several obstacles that need to be overcome before the possibilities offered by these
212 genomes can be fully exploited. The main bottleneck is the lack of an efficient and reproducible
213 protocol with which targeted genetic manipulations can be performed. Previous attempts to
214 transform *Cuscuta* have shown that *A. tumefaciens* is able to transform callus cells (Borsics et al.,
215 2002; Svbova and Blehova, 2013). However, in our hands these transformation events were
216 very scarce, explaining maybe why this approach has not yielded greater success.

217 With the work presented here, we show that transformation of *Cuscuta reflexa* works very
218 efficiently when developing infection sites are targeted. As our experiments show, the protocol
219 works with both, *A. rhizogenes* and *A. tumefaciens* and allows the expression of reporter proteins
220 from different binary vectors and under the control of different promoters. The T-DNA of
221 pRedRoot, a binary vector developed for *A. rhizogenes*, contains the dsRed protein under control
222 of the Ubi10 promoter (Libiakova et al., 2018), while the *A. tumefaciens* line used by Bobik et al.
223 (2019) contains a GFP gene controlled by the 35S promoter. Both promoters allow strong

224 constitutive expression of transgenes. It remains to be shown if other - in particular inducible -
225 promoters work in *Cuscuta* as well as the standard constitutive promoters do, or if adaptations are
226 required for use with the parasite.

227 The simplicity of the method (low-tech, cheap and easy-to-learn) (Fig. 1) and the high
228 reproducibility makes it suitable for larger-scale screening approaches. The high numbers of
229 transformed cells and the longevity of transgene expression are good preconditions for the
230 development of a callus culture that can then be used to regenerate transgenic *Cuscuta* plants.

231 The high transformation rates of adhesive disk cells is certainly noteworthy. Agrobacteria are
232 known to be attracted to polyphenolic substances exuded by plant roots (Ozyigit et al., 2013).
233 Haustorial sites are also rich in hydroxycinnamic acid derivatives, caffeic acid depsides and other
234 polyphenols (Löffler et al., 1995), which is evident by the rapid browning of infection sites upon
235 their exposure to air (Johnsen et al., 2015). Comparably high concentrations of phenolic
236 substances, albeit in a slightly different composition, are interestingly also found in the
237 meristematic apex of *Cuscuta* shoots (Löffler et al., 1995). After adhesive disks, shoot tips were
238 the second tissue that showed a heightened susceptibility towards agrobacterial infection.
239 However, attraction by polyphenols does not explain why only the adhesive disks and not the
240 haustoria are transformed as the latter exhibit high phenolic substance production as well (Löffler
241 et al., 1995). Both haustoria and the surrounding adhesive disks are characterized by a high
242 metabolic activity, so that limiting rates of transcription and translation are not likely to be the
243 cause for the lack of transgene expression in the haustorium. The life cell stain CFDA that
244 indicates accessibility and viability of stained cells was also detected in both organs (Fig. 3),
245 albeit with a preference for adhesive disks over haustoria. Stems, in contrast were not stained.
246 The presence (in stems) or absence (in infection sites) of a cuticle supposedly determines how
247 rapidly the stain is absorbed. The cuticle could likewise be effective in reducing access to cells
248 for agrobacteria. However, even with these explanations, it remains a mystery why the adhesive

249 disks show high transformation rates while the haustoria are not transformed at all, and this
250 certainly deserves further investigations in the future.

251 None of the species that belong to the genus *Cuscuta* possesses roots and they are therefore no
252 obvious natural targets of the plant pathogenic bacterium *Agrobacterium rhizogenes*.
253 Nevertheless, some *Cuscuta* species were recently shown to have acquired a gene coding for the
254 Mikimopine synthase (*mis* gene) (Zhang et al., 2020) that is typically transferred to plants during
255 *A. rhizogenes* infection in order to supply the bacterium with opines. Plant homologues of the *mis*
256 gene are found only in a handful of plant species belonging to the genera *Nicotiana* and *Linnaria*
257 where they are believed to have originated by three independent horizontal gene transfer (HGT)
258 events (Kovacova et al., 2014). These species do not display the hairy root syndrome, which
259 hypothetically could be attributed to the HGT-derived *mis* gene. By way of small interfering
260 RNAs from the HGT-derived *mis* that may degrade T-DNA-borne *mis* transcripts during an
261 infection, these acquired genes could potentially prevent *A. rhizogenes* growth. Their evolution
262 under selective pressure and the coverage of *mis*-derived siRNAs, at least, seem to corroborate
263 this possibility for *Nicotiana* (Kovacova et al., 2014). It can be debated whether this could also be
264 the case in *Cuscuta*. However, the *mis* gene was so far only found in species belonging to the
265 subgenus *Grammica* (Zhang et al., 2020), but was not detected in a transcriptome database (Olsen
266 et al., 2016) of *C. reflexa*. Therefore, it is more likely that the loss of key genes involved in root
267 development is responsible for the failure to produce hairy roots in *A. rhizogenes*-infected
268 *Cuscuta* tissue.

269

270 CONCLUSIONS

271 Using fluorescent reporter proteins and far-red light mediated infection structure induction, we
272 have shown that the adhesive disk of *C. reflexa* is highly susceptible to *Agrobacterium*-mediated
273 transformation. With the high number of transformation events that were observed using our

274 protocol and with the stability of transgene expression, it will be possible to perform
275 transformations with a high number of constructs. Applications of this protocol are, among
276 others, protein localization studies, protein interaction studies (using the high co-transformation
277 rates) and expression of heterologous or synthetic transgenes. Moreover, if the transformed cells
278 can be induced to produce callus and ultimately whole regenerated plants, it will finally be
279 possible to harness the genome sequence information and create *Cuscuta* mutants.

280

281 MATERIALS AND METHODS

282 Plant material and *Agrobacterium* strains

283 *Cuscuta reflexa*, *Cuscuta campestris* and *Cuscuta platyloba* were grown in a greenhouse on the
284 host *Pelargonium zonale* under continuous illumination and a constant temperature of 21 °C
285 (Förste et al., 2019). The bacteria and binary T-DNA-containing vectors pRedRoot and XM82,
286 respectively, were kindly contributed by Prof. Harro Bouwmeester (University of Amsterdam,
287 Netherlands) (*A. rhizogenes*) and Prof. Tessa Burch-Smith (University of Tennessee, USA) (*A.*
288 *tumefaciens*) and are described in more detail in other studies (Limpens et al., 2004; Libiakova et
289 al., 2018; Bobik et al., 2019). Cultures of *A. rhizogenes* MSU440 and *A. tumefaciens* GV3101
290 without binary plasmids were grown on LB medium (tryptone 10 g/L, NaCl 10 g/L, yeast extract
291 5 g/L, agar 7,5 g/L) supplemented with 100 mg/L Spectinomycin or 50 mg/L Rifampicin plus 50
292 mg/L Gentamycin, respectively. For bacteria containing the respective binary vectors,
293 Kanamycin at 50 µg/ml was added to the growth medium.

294

295 Induction of infection structure formation by far-red light

296 For induction of infection structures, *Cuscuta* apical shoots of approximately 12 cm were
297 harvested from the stock plant and exposed to far red light (740 nm) in an otherwise dark room
298 for 90-120 minutes as described before (Olsen et al., 2016) with modifications. The steps were

299 conducted in far red light to not reverse the induction (Tada et al., 1996). To provide a tactile
300 stimulus, four shoots of roughly equal diameter were placed next to each other between two
301 layers of bench paper with one-sided plastic coating (Whatman® Benchkote® surface protector;
302 Cat. # 2300731) that was moistened with tap water (filter-paper side facing the shoots). This set-
303 up was carefully placed between two back-to-back facing petri dish halves (with the filter paper
304 and the cut ends both protruding into a container with tap water (see Fig. 1). Moderate pressure
305 was applied by taping the two petri dish plates together. When kept at room temperature in
306 darkness, infection structures started to develop after about three days (Olsen et al., 2016).

307

308 **Transformation of *Cuscuta* cells**

309 An *Agrobacterium* culture was grown overnight in selective media (see above) and adjusted to an
310 OD (595 nm) of 1 to 1.6, before using 2 ml of this suspension to soak the paper side of the bench
311 paper (approximately 8x8 cm area). For mock controls, agrobacteria lacking a T-DNA-encoding
312 binary vector were used. The assembly with far red light-treated *Cuscuta* stems was done as
313 described above and the whole setup was then incubated in a dark incubator set to room
314 temperature for seven days. After disassembling the setup, shoots were briefly rinsed under tap
315 water, remnants of filter paper sticking to the adhesive disks were carefully removed without
316 damaging the plant tissue and stems were kept for up to two days in water or wrapped in wet
317 paper towels before being subjected to microscopical analysis.

318 For exchange of water to *Agrobacterium* culture and *vice versa* (see Supplemental tables), the
319 setup was disassembled on day 3 under far red light (740 nm) and the bench paper layer
320 exchanged before the setup was re-assembled and subjected to further incubation in the dark for
321 another five days.

322

323 **Microscopical imaging**

324 Fluorescence localization in the *Cuscuta* stems exposed to agrobacteria and in the corresponding
325 controls was documented using a StereoLumar V12 stereo microscope or an Axiovert M200
326 inverted microscope (both from Zeiss) using Zeiss filter sets 43 (for dsRed) and 38 (for GFP).
327 Images were taken using the Axiovision Software (Version 4.8.2). The same exposure times were
328 used for the different fluorescence filter sets for a given sample or magnification, unless specified
329 otherwise. FIJI/ImageJ (V 2.0.0) was used to analyze the pictures, add scalebars, and produce
330 overlays. When adjusting brightness, contrast, minimum and maximum intensities, all
331 fluorescence images of one set were treated alike.

332 Fluorescence intensity scanning was performed on the marked area containing the region of
333 interest (see Supplemental Fig. S4) using the histogram function of FIJI/ImageJ. Intensity counts
334 were exported to Microsoft Excel for visualization in one joint colored graph.

335

336 **Vibratome sectioning**

337 Transformed infection sites were cross-sectioned using a Vibratome (Leica VT1000 E vibrating
338 blade microtome). Section thickness was 100 μm . Sections were viewed and documented using a
339 StereoLumar V12 stereo microscope or an Axiovert M200 inverted microscope (Zeiss) using
340 Zeiss filter sets 43 (for dsRed) and 38 (for GFP).

341

342 **Life cell staining with 5-carboxyfluorescein di-acetate (CFDA)**

343 To evaluate the vitality of the transformed cells, the vital stain CFDA (50 mM in DMSO) was
344 diluted immediately prior to use to a final working concentration of 1 mM in water. Stems were
345 covered with a thin layer of CFDA by spreading small drops of a few μl each evenly over the
346 *Cuscuta* stem and infection sites (adjusted from “Drop-And-See assay” (Cui et al., 2015)). After

347 incubation for 10 minutes in the dark, the stems were rinsed with tap water, gently dried with
348 paper and viewed under a StereoLumar V12 stereo microscope using Zeiss filter set 38.

349

350 **Cultivation of explants**

351 *Cuscuta reflexa* stems with infection sites and confirmed transformation events were sterilized
352 for 2-5 minutes in 70 % Ethanol and during this time gently cleaned using a brush. After a
353 subsequent 15 minutes incubation step in 1.2 % Sodiumhypochloride, the stems were incubated
354 on a shaker in sterile tap water containing 400 mg/L Cefotaxime overnight, then cut into pieces
355 that contained one or two infection structures each and transferred to MS (Murashige and Skoog)
356 Basal Medium supplemented with 0.8 % Agar, 3 % Sucrose, MS Vitamin solution and 400 mg/L
357 Cefotaxime. Plates were covered with aluminum foil to avoid photobleaching and were kept at 23
358 °C. Explants were transferred to fresh medium approximately every 4 weeks.

359

360 **ACKNOWLEDGEMENTS**

361 This work is part of the doctoral thesis of LL. Financial support from the Tromsø Research
362 Foundation (Mohn Foundation) (grant 16-TF-KK to KK) and the Department of Arctic and
363 Marine Biology (AMB, UiT The Arctic University of Norway) is gratefully acknowledged. We
364 thank Prof. Harro Bouwmeester (University of Amsterdam, Netherlands) for stimulating
365 discussions that provided the initial impulse to this study. We further thank the “Norway-
366 Armenia cooperation in plant molecular biology and biotechnology for agricultural development”
367 project (CPEA-LT-2016/10092), funded by the Eurasia program, Norwegian Agency for
368 International Cooperation and Quality Enhancement in Higher Education (DIKU) for supporting
369 the research visit of LG to Tromsø. Staff at the Climate Laboratory Holt (especially Leidulf
370 Lund) is thanked for *Cuscuta* maintenance. *Agrobacterium* strains and binary reporter plasmids
371 were kindly provided by Prof. Tessa Burch-Smith (University of Tennessee, USA) and Prof.

372 Harro Bouwmeester (University of Amsterdam, Netherlands). Prof. Karsten Fischer and Dr. Stian
373 Olsen (both from UiT The Arctic University of Tromsø, Norway) have contributed with
374 numerous suggestions and discussions to the work and the manuscript.

375

376

377 LITERATURE CITED

378 **Alagarsamy K, Shamala LF, Wei S** (2018) Protocol: high-efficiency in-planta *Agrobacterium*-
379 mediated transgenic hairy root induction of *Camellia sinensis* var. *sinensis*. *Plant Meth*
380 **14:** 17

381 **Bahramnejad B, Naji M, Bose R, Jha S** (2019) A critical review on use of *Agrobacterium*
382 *rhizogenes* and their associated binary vectors for plant transformation. *Biotechnol Adv*
383 **37:** 107405

384 **Bobik K, Fernandez JC, Hardin SR, Ernest B, Ganusova EE, Staton ME, Burch-Smith TM**
385 (2019) The essential chloroplast ribosomal protein uL15c interacts with the chloroplast
386 RNA helicase ISE2 and affects intercellular trafficking through plasmodesmata. *New*
387 *Phytol* **221:** 850-865

388 **Borsics T, Mihalka V, Oreifig AS, Barany I, Lados M, Nagy I, Jenes B, Toldi O** (2002)
389 Methods for genetic transformation of the parasitic weed dodder (*Cuscuta trifolii* Bab. et
390 Gibbs) and for PCR-based detection of early transformation events. *Plant Sci* **162:** 193-199

391 **Cui W, Wang X, Lee JY** (2015) Drop-AND-See: a simple, real-time, and noninvasive technique
392 for assaying plasmodesmal permeability. *Methods Mol Biol* **1217:** 149-156

393 **Förste F, Mantouvalou I, Kanngiesser B, Stosnach H, Lachner LA, Fischer K, Krause K**
394 (2019) Selective mineral transport barriers at *Cuscuta*-host infection sites. *Physiol Plant*
395 **doi: 10.1111/ppl.13035**

396 **Galloway AF, Knox P, Krause K** (2020) Sticky mucilages and exudates of plants: putative
397 microenvironmental design elements with biotechnological value. *New Phytol* **225:** 1461-
398 1469

399 **Gelvin SB** (2003) *Agrobacterium*-mediated plant transformation: the biology behind the "gene-
400 jockeying" tool. *Microbiol Mol Biol Rev* **67:** 16-37

401 **Ho-Plagaro T, Huertas R, Tamayo-Navarrete MI, Ocampo JA, Garcia-Garrido JM** (2018)
402 An improved method for *Agrobacterium rhizogenes*-mediated transformation of tomato
403 suitable for the study of arbuscular mycorrhizal symbiosis. *Plant Meth* **14:** 34

404 **Johnsen HR, Striberry B, Olsen S, Vidal-Melgosa S, Fangel JU, Willats WG, Rose JK,**
405 **Krause K** (2015) Cell wall composition profiling of parasitic giant dodder (*Cuscuta*
406 *reflexa*) and its hosts: a priori differences and induced changes. *New Phytologist* **207:**
407 805-816

408 **Kaiser B, Vogg G, Furst UB, Albert M** (2015) Parasitic plants of the genus *Cuscuta* and their
409 interaction with susceptible and resistant host plants. *Front Plant Sci* **6:** 45

410 **Kovacova V, Zluvova J, Janousek B, Talianova M, Vyskot B** (2014) The evolutionary fate of
411 the horizontally transferred agrobacterial mikimopine synthase gene in the genera
412 *Nicotiana* and *Linaria*. *PLoS One* **9:** e113872

413 **Lee KB** (2007) Structure and development of the upper haustorium in the parasitic flowering
414 plant *Cuscuta japonica* (Convolvulaceae). *Am J Bot* **94:** 737-745

415 **Libiakova D, Ruyter-Spira C, Bouwmeester HJ, Matusova R** (2018) *Agrobacterium*
416 *rhizogenes* transformed calli of the holoparasitic plant *Phelipanche ramosa* maintain
417 parasitic competence. *Plant Cell Tiss Organ Cult* **135:** 321-329

418 **Limpens E, Ramos J, Franken C, Raz V, Compaan B, Franssen H, Bisseling T, Geurts R**
419 (2004) RNA interference in *Agrobacterium rhizogenes*-transformed roots of *Arabidopsis*
420 and *Medicago truncatula*. *J Exp Bot* **55:** 983-992

421 **Löffler C, Sahm A, Wray V, Czygan F-C, Proksch P** (1995) Soluble phenolic constituents
422 from *Cuscuta reflexa* and *Cuscuta platyloba*. *Biochem Syst Ecol* **23:** 121-128

423 **Nagar R, Singh M, Sanwal GG** (1984) Cell wall degrading enzymes in *Cuscuta reflexa* and its
424 hosts. *J Exp Bot* **35:** 8

425 **Olsen S, Striberny B, Hollmann J, Schwacke R, Popper Z, Krause K** (2016) Getting ready
426 for host invasion: elevated expression and action of xyloglucan endotransglucosylases /
427 hydrolases in developing haustoria of the holoparasitic angiosperm *Cuscuta*. *J Exp Bot*
428 **67**: 695-708

429 **Ozyigit II, Dogan I, Tarhan EA** (2013) *Agrobacterium rhizogenes*-mediated transformation and
430 its biotechnological applications in crops. In KR Hakeem, P Ahmad, M Ozturk, eds, *Crop*
431 *Improvement*. Springer Science + Business Media, New York Dordrecht Heidelberg
432 London, pp 1-48

433 **Ron M, Kajala K, Pauluzzi G, Wang D, Reynoso MA, Zumstein K, Garcha J, Winte S,**
434 **Masson H, Inagaki S, Federici F, Sinha N, Deal RB, Bailey-Serres J, Brady SM**
435 (2014) Hairy root transformation using *Agrobacterium rhizogenes* as a tool for exploring
436 cell type-specific gene expression and function using tomato as a model. *Plant Physiol*
437 **166**: 455-469

438 **Shimizu K, Aoki K** (2019) Development of Parasitic Organs of a Stem Holoparasitic Plant in
439 Genus *Cuscuta*. *Front Plant Sci* **10**: 1435

440 **Sun G, Xu Y, Liu H, Sun T, Zhang J, Hettenhausen C, Shen G, Qi J, Qin Y, Li J, Wang L,**
441 **Chang W, Guo Z, Baldwin IT, Wu J** (2018) Large-scale gene losses underlie the
442 genome evolution of parasitic plant *Cuscuta australis*. *Nat Commun* **9**: 2683

443 **Svubova R, Blehova A** (2013) Stable transformation and actin visualization in callus cultures of
444 dodder (*Cuscuta europaea*). *Biologia* **68**: 633-640

445 **Tada Y, M. S, Furuhashi K** (1996) Haustoria of *Cuscuta japonica*, a holoparasitic flowering
446 plant, are induced by the cooperative effects of raf-red light and tactile stimuli. *Plant Cell*
447 *Physiol* **37**: 1049-1053

448 **Vaughn KC** (2002) Attachment of the parasitic weed dodder to the host. *Protoplasma* **219**: 227-
449 237

450 **Vogel A, Schwacke R, Denton AK, Usadel B, Hollmann J, Fischer K, Bolger A, Schmidt**
451 **MH, Bolger ME, Gundlach H, Mayer KFX, Weiss-Schneeweiss H, Temsch EM,**
452 **Krause K** (2018) Footprints of parasitism in the genome of the parasitic flowering plant
453 *Cuscuta campestris*. *Nat Commun* **9**: 2515

454 **Yuncker TG** (1932) The genus *Cuscuta*. *Memoirs of the Torrey Botanical Club* **18**: 113-331

455 **Zhang Y, Wang D, Wang Y, Dong H, Yuan Y, Yang W, Lai D, Zhang M, Jiang L, Li Z**
456 (2020) Parasitic plant dodder (*Cuscuta* spp.): A new natural *Agrobacterium*-to-plant
457 horizontal gene transfer species. *Sci China Life Sci* **63**: 312-316

458

459 **TABLES**

460 Table 1: Transformation efficiency overview

461

Number of shoots	# infection sites total	# adhesive disks transformed	<i>Agrobacterium</i> strain	Reporter fluorochrome
6	61	46	<i>A. rhizogenes</i> MSU440	dsRed
4	16	13	<i>A. rhizogenes</i> MSU440	dsRed
6	37	33	<i>A. rhizogenes</i> MSU440	dsRed
4	77	37	<i>A. rhizogenes</i> MSU440	dsRed
8	41	11	<i>A. rhizogenes</i> MSU440	dsRed
12	57	38	<i>A. rhizogenes</i> MSU440	dsRed
12	137	43	<i>A. rhizogenes</i> MSU440	dsRed
3	21	11	<i>A. tumefaciens</i> GV3101	GFP
3	25	8	<i>A. tumefaciens</i> GV3101	GFP
8	63	15	<i>A. tumefaciens</i> GV3101	GFP
8	52	15	<i>A. tumefaciens</i> GV3101	GFP
8	113	74	<i>A. tumefaciens</i> GV3101	GFP
8	93	49	<i>A. tumefaciens</i> GV3101	GFP
5	38	0	<i>A. rhizogenes</i> MSU440	None
4	28	0	<i>A. rhizogenes</i> MSU440	None
4	50	0	<i>A. rhizogenes</i> MSU440	None

462

463 **FIGURE LEGENDS**

464 **Figure 1:** Overview of the experimental setup. A, Exposure of *Cuscuta* shoots to far red light
465 (740 nm) for 90-120 min. B, Placement of *Cuscuta* shoots between *Agrobacterium*-soaked bench
466 paper sheets and two petri dish halves (back to back). C, Incubation in darkness with shoots and
467 bench paper placed in a water reservoir.

468

469 **Figure 2:** Transformation of *C. reflexa* adhesive disks by *A. rhizogenes* containing the binary
470 vector pRedRoot. A-F, Intact infection sites after transformation. Topview (A-C) and sideview
471 (D-F) of transformed adhesive disks are shown. G-L, Semithin vibratome sections of transformed
472 adhesive disk tissue showing sub-epidermal localization of transformed cells. M-N, Mock
473 transformation with *A. rhizogenes* lacking the binary pRedRoot plasmid. Darkfield or brightfield
474 pictures (first column) are shown alongside the fluorescence images taken with a Cy3 filter
475 (middle column). Overlays of both are shown in the right column. Adhesive disks (ad) and
476 haustoria (h) are indicated. Scale bars are 1000 μ m (C, I), 2000 μ m (F, N) and 100 μ m (L).

477

478 **Figure 3:** Uptake of 5-Carboxyfluorescein-diacetate (CFDA) into adhesive disks of *C. reflexa*.
479 A-C, Green CFDA fluorescence is shown in a shoot segment containing two developing infection
480 sites. A superimposition of the images from A and B is shown in C. D-F, CFDA uptake into an
481 adhesive disk containing dsRed-expressing cells. Darkfield images (left column) and
482 fluorescence images (middle column and lower right image) are shown. Adhesive disks (ad) and
483 haustoria (h) are indicated. Scale bars are 1000 μ m.

484

485 **Figure 4:** Extension of the protocol to *A. tumefaciens* and *C. campestris*. A-F, Negative (A-C)
486 and positive (D-F) controls using the combination of *C. reflexa* and *A. rhizogenes* (see also Fig.
487 2). G-I, Transformation after combining *C. reflexa* with *A. tumefaciens* containing a binary GFP-
488 expressing vector. J-O, Negative control (J-L) and pRedRoot transformation (M-O) using the
489 combination of *C. campestris* and *A. rhizogenes*. Scalebars represent 2000 µm (C, F, I, O) and
490 1000 µm (L), respectively. White fibres of the bench paper from the experimental setup can be
491 seen adhering strongly to the adhesive disks in some darkfield images (D, G, J, M).

492

493 **Figure 5:** Co-transformation of different reporter proteins in *C. reflexa* adhesive disks. DsRed
494 was introduced with *A. rhizogenes* while GFP was introduced with *A. tumefaciens*. A-D, Side
495 view of intact stem with darkfield (A), red fluorescence (B) and green fluorescence (C) images. D
496 shows a superimposed image of the two fluorescence images with thick arrows pointing at spots
497 where both reporter proteins coincide (yellow color due to overlay). The scalebar measures 1000
498 µm. E-H, Cross section through a transformed infection site with darkfield (E), red fluorescence
499 (F) and green fluorescence (G) images. H shows a superimposed image of all three images. The
500 scalebar measures 500 µm. The asterisk and the arrowhead indicate cells that are transformed
501 with only one reporter protein. The thick arrow indicates cells were both reporter proteins
502 coincide. I, Intensity scan performed on the two single fluorescent images with the purple line
503 representing the dsRed fluorescence and the green line representing the GFP fluorescence.

504

505 **Figure 6:** Cultivation of pRedRoot-expressing explants from *C. reflexa*. The shown explant
506 contains two infection structures with transformed adhesive disks. Asterisks indicate clusters of
507 transformed cells. Images were taken after 5 days (A-B) and 4 weeks (C-D) in sterile culture.
508 Brightfield images are shown next to the red fluorescence. The scalebars represent 1000 µm.

509

510 **SUPPLEMENTARY INFORMATION**

511 The following supplemental materials are available:

512 **Supplemental Table 1:** Transformation efficiency in *C. reflexa* shoots when *Agrobacterium*
513 solution was replaced with water on day 3 of infection structure induction.

514 **Supplemental Table 2:** Transformation efficiency in *C. reflexa* shoots when *Agrobacterium*
515 solution was added on day 3 of infection structure induction.

516 **Supplemental Figure S1.** Examples for infrequent events of transformation in shoot tip and
517 stem.

518 **Supplemental Figure S2.** Specific fluorescence and autofluorescence of an adhesive disk
519 transformed with *A. rhizogenes* carrying the binary plasmid pRedRoot.

520 **Supplemental Figure S3.** Localization of GFP expressing cells in semi-thin adhesive disk
521 sections of *C. reflexa* upon transformation with *A. tumefaciens*.

522 **Supplemental Figure S4.** Area used for intensity-scanning of the images taken of a co-
523 transformed adhesive disk (related to Fig. 5I).

524

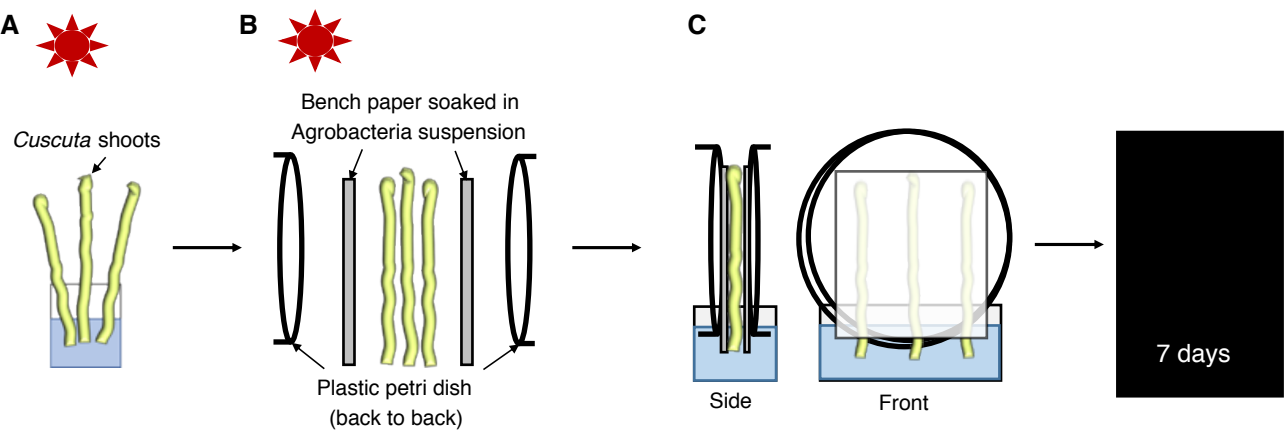


Figure 1: Overview of the experimental setup. A, Exposure of *Cuscuta* shoots to far red light (740 nm) for 90-120 min. B, Placement of *Cuscuta* shoots between *Agrobacterium*-soaked bench paper sheets and two petri dish halves (back to back). C, Incubation in darkness with shoots and bench paper placed in a water reservoir.

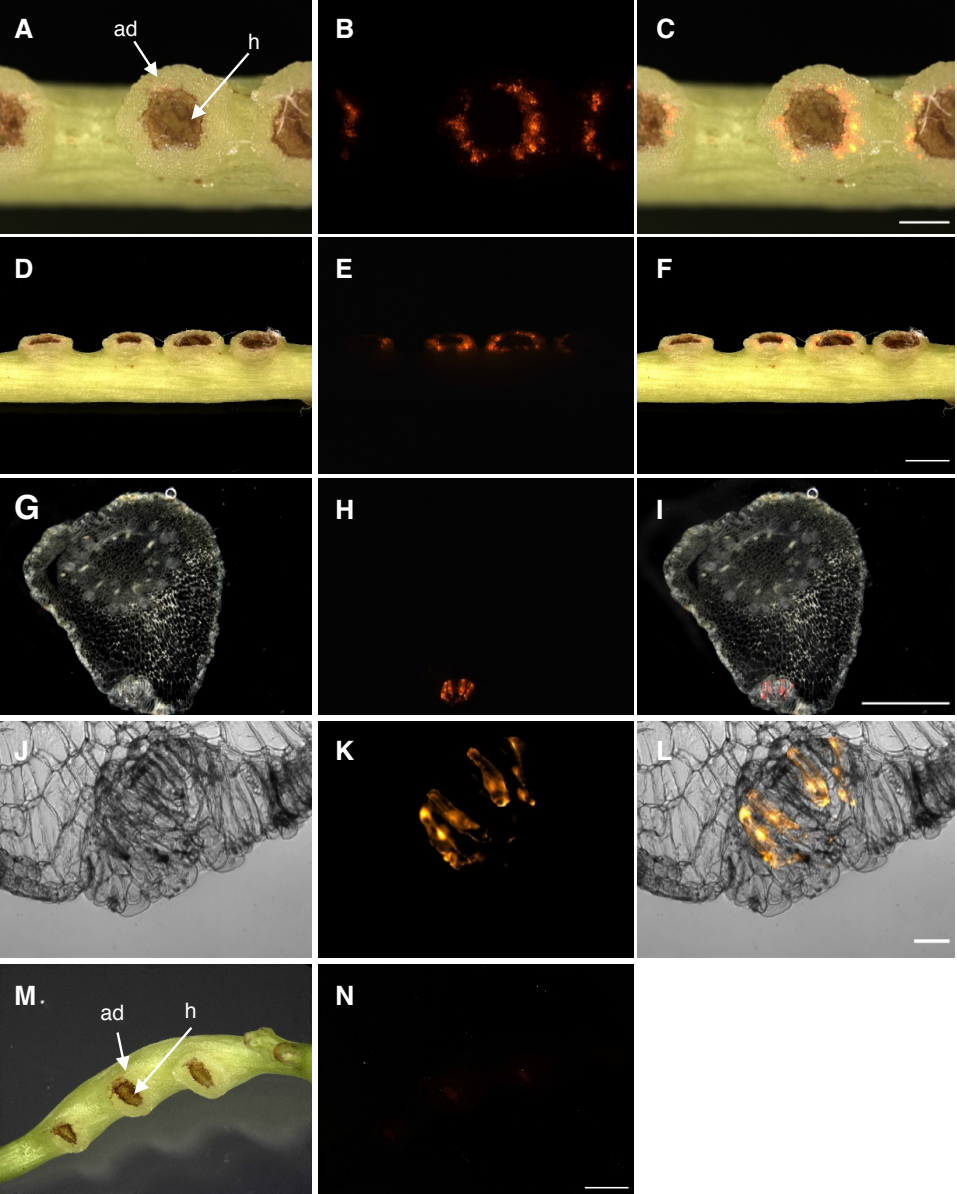


Figure 2: Transformation of *C. reflexa* adhesive disks by *A. rhizogenes* containing the binary vector pRedRoot. A-F, Intact infection sites after transformation. Topview (A-C) and sideview (D-F) of transformed adhesive disks are shown. G-L, Semithin vibratome sections of transformed adhesive disk tissue showing sub-epidermal localization of transformed cells. M-N, Mock transformation with *A. rhizogenes* lacking the binary pRedRoot plasmid. Darkfield or brightfield pictures (first column) are shown alongside the fluorescence images taken with a Cy3 filter (middle column). Overlays of both are shown in the right column. Adhesive disks (ad) and haustoria (h) are indicated. Scale bars are 1000 μ m (C, I), 2000 μ m (F, N) and 100 μ m (L).

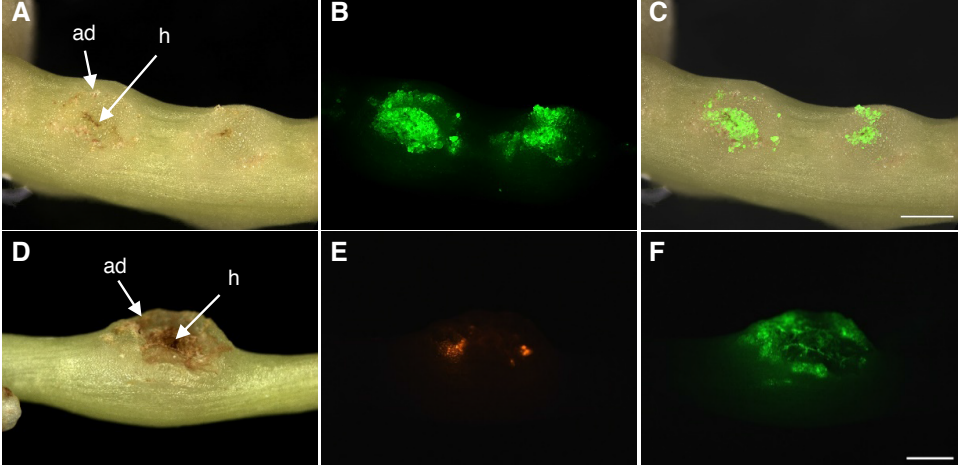


Figure 3: Uptake of 5-Carboxyfluorescein-diacetate (CFDA) into adhesive disks of *C. reflexa*. A-C, Green CFDA fluorescence is shown in a shoot segment containing two developing infection sites. A superimposition of the images from A and B is shown in C. D-F, CFDA uptake into an adhesive disk containing dsRed-expressing cells. Darkfield images (left column) and fluorescence images (middle column and lower right image) are shown. Adhesive disks (ad) and haustoria (h) are indicated. Scale bars are 1000 μ m.

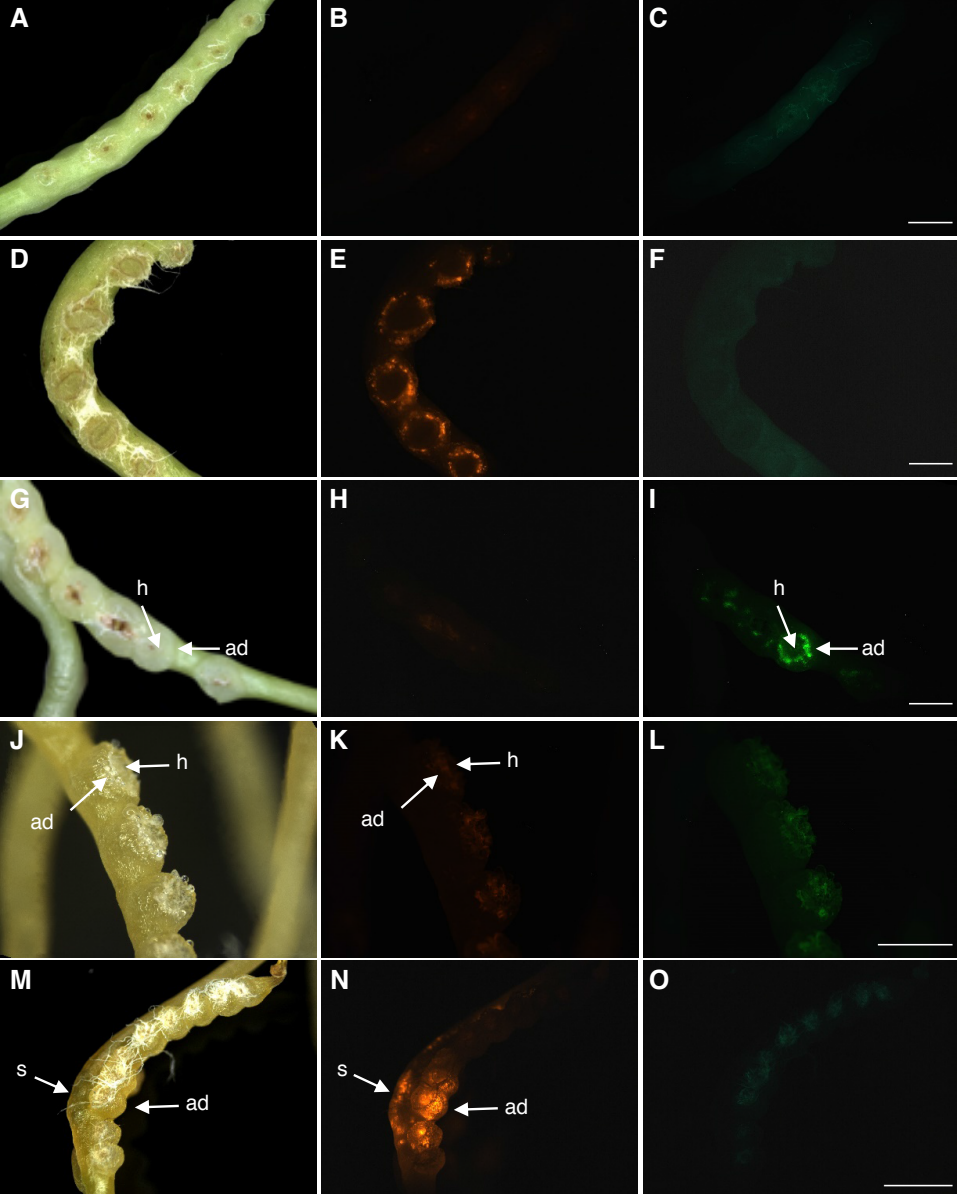


Figure 4: Extension of the protocol to *A. tumefaciens* and *C. campestris*. A-F, Negative (A-C) and positive (D-F) controls using the combination of *C. reflexa* and *A. rhizogenes* (see also Fig. 2). G-I, Transformation after combining *C. reflexa* with *A. tumefaciens* containing a binary GFP-expressing vector. J-O, Negative control (J-L) and pRedRoot transformation (M-O) using the combination of *C. campestris* and *A. rhizogenes*. Scalebars represent 2000 μ m (C, F, I, O) and 1000 μ m (L), respectively. White fibres of the bench paper from the experimental setup can be seen adhering strongly to the adhesive disks in some darkfield images (D, G, J, M).

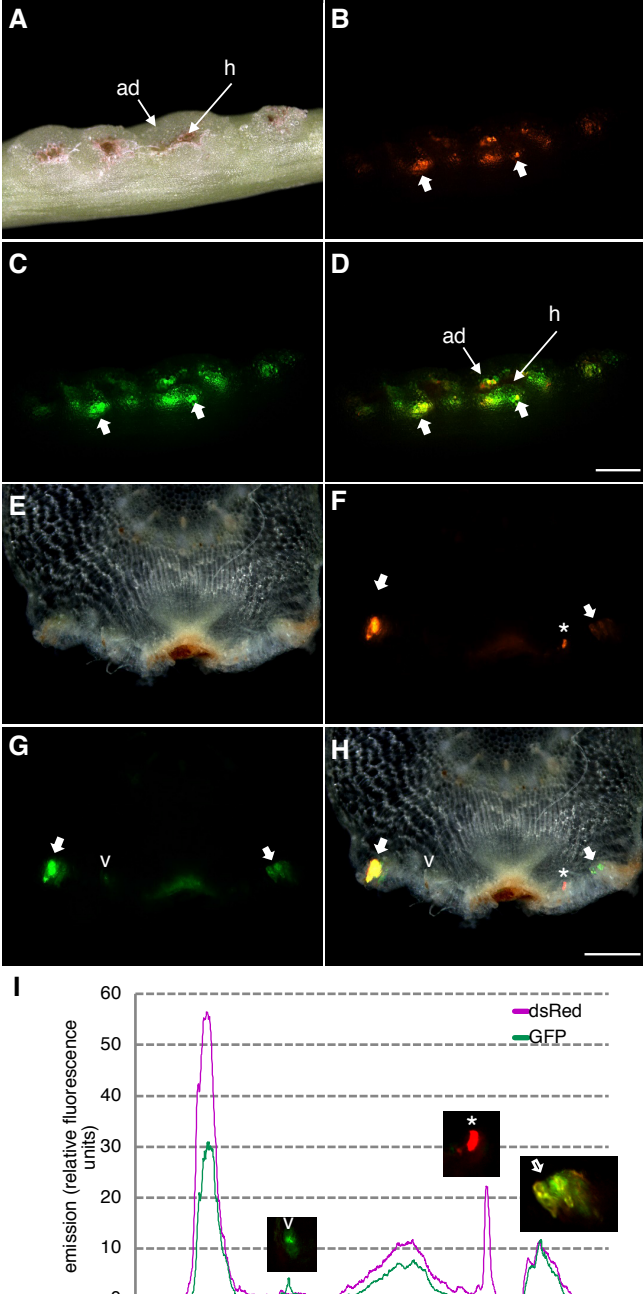


Figure 5: Co-transformation of different reporter proteins in *C. reflexa* adhesive disks. DsRed was introduced with *A. rhizogenes* while GFP was introduced with *A. tumefaciens*. A-D, Side view of intact stem with darkfield (A), red fluorescence (B) and green fluorescence (C) images. D shows a superimposed image of the two fluorescence images with thick arrows pointing at spots where both reporter proteins coincide (yellow color due to overlay). The scalebar measures 1000 μ m. E-H, Cross section through a transformed infection site with darkfield (E), red fluorescence (F) and green fluorescence (G) images. H shows a superimposed image of all three images. The scalebar measures 500 μ m. The asterisk and the arrowhead indicate cells that are transformed with only one reporter protein. The thick arrow indicates cells were both reporter proteins coincide. I, Intensity scan performed on the two single fluorescent images with the purple line representing the dsRed fluorescence and the green line representing the GFP fluorescence.

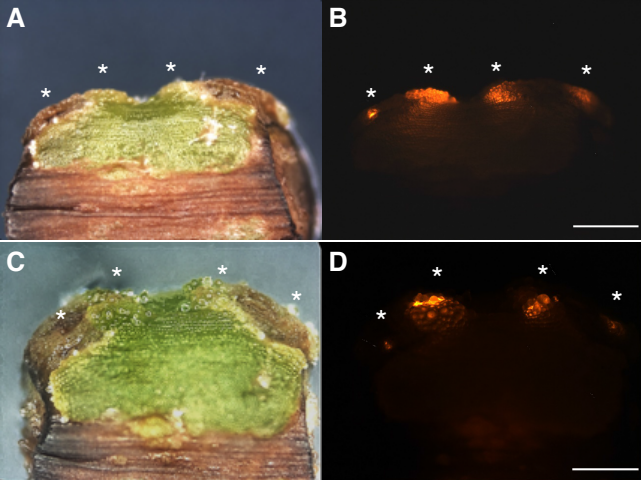


Figure 6: Cultivation of pRedRoot-expressing explants from *C. reflexa*. The shown explant contains two infection structures with transformed adhesive disks. Asterisks indicate clusters of transformed cells. Images were taken after 5 days (A-B) and 4 weeks (C-D) in sterile culture. Brightfield images are shown next to the red fluorescence. The scalebars represent 1000 μ m.

Parsed Citations

Alagarsamy K, Shamala LF, Wei S (2018) Protocol: high-efficiency in-planta Agrobacterium-mediated transgenic hairy root induction of *Camellia sinensis* var. *sinensis*. *Plant Meth* 14: 17

Pubmed: [Author and Title](#)

Google Scholar: [Author Only](#) [Title Only](#) [Author and Title](#)

Bahramnejad B, Naji M, Bose R, Jha S (2019) A critical review on use of *Agrobacterium rhizogenes* and their associated binary vectors for plant transformation. *Biotechnol Adv* 37: 107405

Pubmed: [Author and Title](#)

Google Scholar: [Author Only](#) [Title Only](#) [Author and Title](#)

Bobik K, Fernandez JC, Hardin SR, Ernest B, Ganusova EE, Staton ME, Burch-Smith TM (2019) The essential chloroplast ribosomal protein uL15c interacts with the chloroplast RNA helicase ISE2 and affects intercellular trafficking through plasmodesmata. *New Phytol* 221: 850-865

Pubmed: [Author and Title](#)

Google Scholar: [Author Only](#) [Title Only](#) [Author and Title](#)

Borsics T, Mihalka V, Orefig AS, Barany I, Lados M, Nagy I, Jenes B, Toldi O (2002) Methods for genetic transformation of the parasitic weed dodder (*Cuscuta trifolii* Bab. et Gibbs) and for PCR-based detection of early transformation events. *Plant Sci* 162: 193-199

Pubmed: [Author and Title](#)

Google Scholar: [Author Only](#) [Title Only](#) [Author and Title](#)

Cui W, Wang X, Lee JY (2015) Drop-AND-See: a simple, real-time, and noninvasive technique for assaying plasmodesmal permeability. *Methods Mol Biol* 1217: 149-156

Pubmed: [Author and Title](#)

Google Scholar: [Author Only](#) [Title Only](#) [Author and Title](#)

Förste F, Mantouvalou I, Kanngiesser B, Stosnach H, Lachner LA, Fischer K, Krause K (2019) Selective mineral transport barriers at *Cuscuta*-host infection sites. *Physiol Plant* doi: 10.1111/ppl.13035

Pubmed: [Author and Title](#)

Google Scholar: [Author Only](#) [Title Only](#) [Author and Title](#)

Galloway AF, Knox P, Krause K (2020) Sticky mucilages and exudates of plants: putative microenvironmental design elements with biotechnological value. *New Phytol* 225: 1461-1469

Pubmed: [Author and Title](#)

Google Scholar: [Author Only](#) [Title Only](#) [Author and Title](#)

Gelvin SB (2003) Agrobacterium-mediated plant transformation: the biology behind the "gene-jockeying" tool. *Microbiol Mol Biol Rev* 67: 16-37

Pubmed: [Author and Title](#)

Google Scholar: [Author Only](#) [Title Only](#) [Author and Title](#)

Ho-Plagaro T, Huertas R, Tamayo-Navarrete MI, Ocampo JA, Garcia-Garrido JM (2018) An improved method for Agrobacterium rhizogenes-mediated transformation of tomato suitable for the study of arbuscular mycorrhizal symbiosis. *Plant Meth* 14: 34

Pubmed: [Author and Title](#)

Google Scholar: [Author Only](#) [Title Only](#) [Author and Title](#)

Johnsen HR, Stríberny B, Olsen S, Vidal-Melgosa S, Fangel JU, Willats WG, Rose JK, Krause K (2015) Cell wall composition profiling of parasitic giant dodder (*Cuscuta reflexa*) and its hosts: a priori differences and induced changes. *New Phytologist* 207: 805-816

Pubmed: [Author and Title](#)

Google Scholar: [Author Only](#) [Title Only](#) [Author and Title](#)

Kaiser B, Vogg G, Furst UB, Albert M (2015) Parasitic plants of the genus *Cuscuta* and their interaction with susceptible and resistant host plants. *Front Plant Sci* 6: 45

Pubmed: [Author and Title](#)

Google Scholar: [Author Only](#) [Title Only](#) [Author and Title](#)

Kovacova V, Zluvova J, Janousek B, Talianova M, Vyskot B (2014) The evolutionary fate of the horizontally transferred agrobacterial *mikimopine synthase* gene in the genera *Nicotiana* and *Linaria*. *PLoS One* 9: e113872

Pubmed: [Author and Title](#)

Google Scholar: [Author Only](#) [Title Only](#) [Author and Title](#)

Lee KB (2007) Structure and development of the upper haustorium in the parasitic flowering plant *Cuscuta japonica* (Convolvulaceae). *Am J Bot* 94: 737-745

Pubmed: [Author and Title](#)

Google Scholar: [Author Only](#) [Title Only](#) [Author and Title](#)

Libiakova D, Ruyter-Spira C, Bouwmeester HJ, Matusova R (2018) Agrobacterium rhizogenes transformed calli of the holoparasitic plant *Phelipanche ramosa* maintain parasitic competence. *Plant Cell Tiss Organ Cult* 135: 321-329

Pubmed: [Author and Title](#)

Google Scholar: [Author Only](#) [Title Only](#) [Author and Title](#)

Limpens E, Ramos J, Franken C, Raz V, Compaan B, Franssen H, Bisseling T, Geurts R (2004) RNA interference in Agrobacterium

rhizogenes-transformed roots of *Arabidopsis* and *Medicago truncatula*. *J Exp Bot* 55: 983-992

Pubmed: [Author and Title](#)

Google Scholar: [Author Only Title Only Author and Title](#)

Löffler C, Sahm A, Wray V, Czygan F-C, Proksch P (1995) Soluble phenolic constituents from *Cuscuta reflexa* and *Cuscuta platyloba*. *Biochem Syst Ecol* 23: 121-128

Pubmed: [Author and Title](#)

Google Scholar: [Author Only Title Only Author and Title](#)

Nagar R, Singh M, Sanwal GG (1984) Cell wall degrading enzymes in *Cuscuta reflexa* and its hosts. *J Exp Bot* 35: 8

Pubmed: [Author and Title](#)

Google Scholar: [Author Only Title Only Author and Title](#)

Olsen S, Stríberny B, Hollmann J, Schwacke R, Popper Z, Krause K (2016) Getting ready for host invasion: elevated expression and action of xyloglucan endotransglucosylases / hydrolases in developing haustoria of the holoparasitic angiosperm *Cuscuta*. *J Exp Bot* 67: 695-708

Pubmed: [Author and Title](#)

Google Scholar: [Author Only Title Only Author and Title](#)

Ozyigit II, Dogan I, Tarhan EA (2013) Agrobacterium rhizogenes-mediated transformation and its biotechnological applications in crops. In KR Hakeem, P Ahmad, M Ozturk, eds, *Crop Improvement*. Springer Science + Business Media, New York Dordrecht Heidelberg London, pp 1-48

Pubmed: [Author and Title](#)

Google Scholar: [Author Only Title Only Author and Title](#)

Ron M, Kajala K, Pauluzzi G, Wang D, Reynoso MA, Zumstein K, Garcha J, Winte S, Masson H, Inagaki S, Federici F, Sinha N, Deal RB, Bailey-Serres J, Brady SM (2014) Hairy root transformation using *Agrobacterium rhizogenes* as a tool for exploring cell type-specific gene expression and function using tomato as a model. *Plant Physiol* 166: 455-469

Pubmed: [Author and Title](#)

Google Scholar: [Author Only Title Only Author and Title](#)

Shimizu K, Aoki K (2019) Development of Parasitic Organs of a Stem Holoparasitic Plant in Genus *Cuscuta*. *Front Plant Sci* 10: 1435

Pubmed: [Author and Title](#)

Google Scholar: [Author Only Title Only Author and Title](#)

Sun G, Xu Y, Liu H, Sun T, Zhang J, Hettenhausen C, Shen G, Qi J, Qin Y, Li J, Wang L, Chang W, Guo Z, Baldwin IT, Wu J (2018) Large-scale gene losses underlie the genome evolution of parasitic plant *Cuscuta australis*. *Nat Commun* 9: 2683

Pubmed: [Author and Title](#)

Google Scholar: [Author Only Title Only Author and Title](#)

Svubova R, Blehova A (2013) Stable transformation and actin visualization in callus cultures of dodder (*Cuscuta europaea*). *Biologia* 68: 633-640

Pubmed: [Author and Title](#)

Google Scholar: [Author Only Title Only Author and Title](#)

Tada Y, M. S, Furuhashi K (1996) Haustoria of *Cuscuta japonica*, a holoparasitic flowering plant, are induced by the cooperative effects of raf-red light and tactile stimuli. *Plant Cell Physiol* 37: 1049-1053

Pubmed: [Author and Title](#)

Google Scholar: [Author Only Title Only Author and Title](#)

Vaughn KC (2002) Attachment of the parasitic weed dodder to the host. *Protoplasma* 219: 227-237

Pubmed: [Author and Title](#)

Google Scholar: [Author Only Title Only Author and Title](#)

Vogel A, Schwacke R, Denton AK, Usadel B, Hollmann J, Fischer K, Bolger A, Schmidt MH, Bolger ME, Gundlach H, Mayer KFX, Weiss-Schneeweiss H, Temsch EM, Krause K (2018) Footprints of parasitism in the genome of the parasitic flowering plant *Cuscuta campestris*. *Nat Commun* 9: 2515

Pubmed: [Author and Title](#)

Google Scholar: [Author Only Title Only Author and Title](#)

Yuncker TG (1932) The genus *Cuscuta*. *Memoirs of the Torrey Botanical Club* 18: 113-331

Pubmed: [Author and Title](#)

Google Scholar: [Author Only Title Only Author and Title](#)

Zhang Y, Wang D, Wang Y, Dong H, Yuan Y, Yang W, Lai D, Zhang M, Jiang L, Li Z (2020) Parasitic plant dodder (*Cuscuta* spp.): A new natural *Agrobacterium*-to-plant horizontal gene transfer species. *Sci China Life Sci* 63: 312-316

Pubmed: [Author and Title](#)

Google Scholar: [Author Only Title Only Author and Title](#)